





ARTICLE OPEN



RACK1 is evolutionary conserved in satellite stem cell activation and adult skeletal muscle regeneration

Elisabetta Catalani^{1,7}, Silvia Zecchini^{2,7}, Matteo Giovarelli^{2,7}, Agnese Cherubini¹, Simona Del Quondam¹, Kashi Brunetti¹, Federica Silvestri¹, Paulina Roux-Biejat², Alessandra Napoli², Silvia Rosanna Casati³, Marcello Ceci⁴, Nicla Romano¹ , Silvia Bongiorno⁴, Giorgio Prantera⁴, Emilio Clementi^{2,5,6}, Cristiana Perrotta¹ , Clara De Palma³ and Davide Cervia¹  

© The Author(s) 2022

Skeletal muscle growth and regeneration involves the activity of resident adult stem cells, namely satellite cells (SC). Despite numerous mechanisms have been described, different signals are emerging as relevant in SC homeostasis. Here we demonstrated that the Receptor for Activated C-Kinase 1 (RACK1) is important in SC function. RACK1 was expressed transiently in the skeletal muscle of post-natal mice, being abundant in the early phase of muscle growth and almost disappearing in adult mature fibers. The presence of RACK1 in interstitial SC was also detected. After acute injury in muscle of both mouse and the fruit fly *Drosophila melanogaster* (used as alternative in vivo model) we found that RACK1 accumulated in regenerating fibers while it declined with the progression of repair process. To note, RACK1 also localized in the active SC that populate recovering tissue. The dynamics of RACK1 levels in isolated adult SC of mice, i.e., progressively high during differentiation and low compared to proliferating conditions, and RACK1 silencing indicated that RACK1 promotes both the formation of myotubes and the accretion of nascent myotubes. In *Drosophila* with depleted RACK1 in all muscle cells or, specifically, in SC lineage we observed a delayed recovery of skeletal muscle after physical damage as well as the low presence of active SC in the wound area. Our results also suggest the coupling of RACK1 to muscle unfolded protein response during SC activation. Collectively, we provided the first evidence that transient levels of the evolutionarily conserved factor RACK1 are critical for adult SC activation and proper skeletal muscle regeneration, favoring the efficient progression of SC from a committed to a fully differentiated state.

Cell Death Discovery (2022)8:459; <https://doi.org/10.1038/s41420-022-01250-8>

INTRODUCTION

Adult skeletal muscle retains the capability to increase in size upon hypertrophic stimuli and to regenerate after injury by a hyperplastic process. Although mature muscle cells possess the capacity to self-repair [1, 2], the main process underlying regeneration involves the activity of postnatal resident stem cells, namely satellite cells (SC) [3]. SC play a role also in response to increased muscle load, such as after exercise, and contribute to the efficient growth of adult myofibers. SC are maintained under quiescent conditions, histologically located in a niche environment between the sarcolemma and the basal lamina of the muscle fiber as small spindle-shaped elements. After stimulation, SC cells change their cellular structure, expanding the cytoplasmic portion, including organelles. In parallel, SC proliferate, differentiate and fuse either each other to form new myofibers or with pre-existing fibers to increase their size [3–6]. The new muscle fibers translate for all the sarcomere components. Activated SC can engage both symmetric and asymmetric divisions. Asymmetric division is a key mechanism that allows the maintenance of the

stem cells pool by supporting the balance between self-renewal and differentiation [3–6]. Once regeneration is complete, SC re-enter quiescence and skeletal muscle regains homeostasis.

Cells of myogenic lineage originate from Pax3⁺/Pax7⁺ progenitors which are both downregulated during active myogenesis, when myogenic regulatory factors, such as MyoD and MyoG, are induced. The main cell-intrinsic molecular mechanisms controlling the SC transition from quiescence to activation involve different transcriptional/post-transcriptional, epigenetic, metabolic and proteostatic regulations, including autophagy [4]. Recent discoveries show that SC are a heterogeneous cell population, even within the same tissue, and that their cell fate depends on multiple intrinsic and extrinsic factors derived from the local and/or systemic environment [4]. Despite several mechanisms have been described, many other factors are emerging as relevant for SC self-renewal, activation, proliferation, and commitment in skeletal muscle during the regeneration process.

The Receptor for Activated C-Kinase 1 (RACK1) is a multifaceted member of the tryptophan-aspartate repeat family of scaffold

¹Department for Innovation in Biological, Agro-food and Forest systems (DIBAF), Università degli Studi della Tuscia, largo dell'Università snc, 01100 Viterbo, Italy. ²Department of Biomedical and Clinical Sciences "Luigi Sacco" (DIBIC), Università degli Studi di Milano, via G.B. Grassi 74, 20157 Milano, Italy. ³Department of Medical Biotechnology and Translational Medicine (BioMeTra), Università degli Studi di Milano, via L. Vanvitelli 32, 20129 Milano, Italy. ⁴Department of Ecological and Biological Sciences (DEB), Università degli Studi della Tuscia, largo dell'Università snc, 01100 Viterbo, Italy. ⁵Unit of Clinical Pharmacology, University Hospital "Luigi Sacco"-ASST Fatebenefratelli Sacco, via G.B. Grassi 74, 20157 Milano, Italy. ⁶Scientific Institute IRCCS "Eugenio Medea", via Don Luigi Monza 20, 23842 Bosisio Parini (LC), Italy. ⁷These authors contributed equally: Elisabetta Catalani, Silvia Zecchini, Matteo Giovarelli. ✉email: d.cervia@unitus.it

Received: 1 August 2022 Revised: 3 November 2022 Accepted: 7 November 2022

Published online: 18 November 2022

proteins and shares significant homology to the β subunit of G-proteins [7, 8]. The functional role for RACK1 is to shuttle its binding partners to intracellular sites; however, another key aspect of RACK1 is the modulation of its partners, either promoting or suppressing the activity of bound enzymes. Although it has been initially isolated as a highly conserved intracellular adaptor protein for activated protein kinase C [9, 10], RACK1 was also found in ribosomes and in various sub-cellular structures, including the nucleus and midbody [11–15]. In ribosomes, RACK1 modulates the translation and controls de-novo polypeptide synthesis [8, 13, 16–18]. RACK1 has been also described to regulate key signals in multiple cellular functions including protein degradation, autophagy, proliferation, differentiation, survival, and development [7, 8, 16, 19]. In vascular smooth muscle cells, RACK1 acts on cell proliferation and contraction [20, 21] and is involved in hypertrophic responses in cardiomyocytes [22]. However, little is known about the role of RACK1 in functional and dysfunctional skeletal muscles and its actions during regenerative myogenesis remain under-investigated. An elegant genetic screen in ageing dystrophic muscles of the fruit fly *Drosophila melanogaster* identified RACK1 as one of dystroglycan and dystrophin interactors involved in cellular stress response [23]. RACK1 is also important in myoproteostasis, locomotor function, and longevity in *Drosophila* [24]. In vertebrates, a meta-analysis suggested a central role of multiple pathways, including RACK1, in the short-term atrophy network of skeletal muscle [25].

Muscle regeneration and rejuvenation therapies can benefit from greater knowledge about SC regulation. Using both mouse and *D. melanogaster* models, this latter as an ideal alternative framework to address questions that could not be easily approached with other organisms, we assessed here the expression/function/signaling of RACK1 in SC and its contribution to muscle regeneration after acute injury. Our result demonstrated for the first time that RACK1 is an important evolutionary conserved factor in adult SC differentiation both in vivo and in vitro. Indeed, RACK1 participates in skeletal muscle homeostasis by activating SC and is required for proper myogenesis of damaged skeletal muscle.

RESULTS

Skeletal muscle growth and RACK1 levels

In tibialis anterior (TA) muscles isolated from mice on post-natal days (P) 0–100, the mRNA of RACK1 was highest at P0 and the levels progressively decreased after birth, being very low at P25 and almost undetectable at P100 (Fig. 1A). In the same temporal window, RACK1 protein levels were significantly downregulated (Fig. 1B). Accordingly, transversal and longitudinal sections of TA muscle showed weak sarcoplasmic expression of RACK1 immunofluorescence in P100 mice (Fig. 1C). The post-natal muscle growth phase was characterized by an evident decrease of myofiber-associated RACK1 staining: during neonatal myogenesis (P7), in which muscle growth is sustained by SC proliferation and fusion, RACK1 is highly expressed while during adult myogenesis (after P21), when myofiber growth is less reliant on SC, RACK1 levels were significantly lower (Fig. 1D).

RACK1 expression is up-regulated during SC activation

At P7, RACK1 staining in TA muscle was localized also in some interstitial cells, likely SC, that populate the growing tissue (Fig. 2A). In agreement with the striking connection between RACK1 expression and SC, we thus isolated single myofibers from TA muscle, since the myofiber culture system preserves the myofiber/stem cell association, which is an essential component of the muscle stem cell niche [26]. Immunofluorescence analysis clearly showed RACK1 staining on the periphery of myofibers in cells expressing Pax7⁺ (Fig. 2B), used as a marker for SC pool.

To dissect the expression of RACK1 during myogenesis, we examined primary SC obtained from mice at P25 and cultured in vitro with growth medium (GM). Differentiation of SC was then induced by a mitogen-poor differentiation medium (DM) [27] and monitored by phase microscopy for myotube formation (Supplementary Fig. S1A). As shown in Fig. 2C, transcript levels of RACK1 were detected in proliferating SC (GM) and progressively increased after 24–72 h of DM, concomitantly to MyoD, MyoG and myosin heavy chain (MyHC) myogenic markers [4, 5]. Similar results were obtained in western blot analysis showing that RACK1 protein peaked at 48 h of DM (Fig. 2D). Consistently, basal RACK1 levels in growing myoblasts significantly increased in MyHC-enriched multinucleated myotubes which are progressing towards mature differentiation, with the highest levels reached in fully differentiated myotubes (Fig. 2E).

RACK1 expression changes in mouse skeletal muscle following injury

Accordingly to the modification of RACK1 during myogenesis in vitro, we verified this issue in vivo skeletal muscle. In particular, RACK1 expression in TA muscles of adult mice was monitored during regeneration induced by injection of cardiotoxin (CTX). As shown in Fig. 3A, acute damage led to a significant increase of RACK1 transcript during active regeneration at 5 and 7 days, while RACK1 content declined at 14 days, when the regeneration is almost complete [28]. Immunofluorescence analysis of muscle sections after 7 days CTX damage identified RACK1 accumulation in the centrally nucleated (regenerating) fibers and significantly higher levels of RACK1 were detected in regenerating fibers when compared with non-regenerating/uninjured fibers (Fig. 3B, C). Accordingly, RACK1 co-localized with the embryonal/developmental myosin heavy chain (MyHC-Emb), used as a proxy for regenerating fibers [29], and MyHC-Emb downregulation paralleled RACK1 expression (Fig. 3D). In addition, in the periphery of regenerating myofibers we also found interstitial cells showing co-localization of RACK1 and the Notch ligand Jagged1 (Fig. 3E), a marker for active SC [30, 31].

Acute skeletal muscle injury and RACK1 expression in *D. melanogaster*

Lineal descendants of muscle stem cells, equivalent of vertebrate muscle SC, are present in adult muscle of *Drosophila* as small, unfused cells observed at the surface and in close proximity to the mature muscle fibers [32, 33]. Based on our previous experience and complementary results simultaneously obtained in mouse and *D. melanogaster* models [34], localized stab injury of thorax muscles, i.e., dorsal longitudinal muscle (DLM), was carried out in young-adults (Oregon wild-type strain) using a small needle. Care was taken to restrict damage such that only few muscle fibers were affected and damage could regenerate. Time-course analysis of longitudinal DLM sections revealed that breaks of myofibers and disordered actin filaments were evident up to 3 days after injury although the physically induced wound was reduced in size (Fig. 4A). After 5 days, morphological regeneration was clearly active with the reconstitution of muscle fiber apparatus and the further repair of wound area. Only small remnants of the injury were visible at 10 days, when the actin filament arrangement almost completely recovered; while the damage was undetectable at day 15.

To determine if muscle damage in *Drosophila* recapitulates the results obtained in mice, we repeated these experiments in *Zfh1*>GFP flies that allow to visualize zinc finger transcription factor (*zfh1*) patterns through a UAS-mCD8:GFP reporter. *Zfh1* was shown to identify a population of muscle-associated cells in fly adult with progenitor-like properties [32, 35]. Uninjured DLM of *Zfh1*>GFP contained a small number of *zfh1*-expressing cells (GFP⁺, unfused SC) located peripherally in close proximity to the muscle fiber surface (Fig. 4B). In line with previous reports [32], during

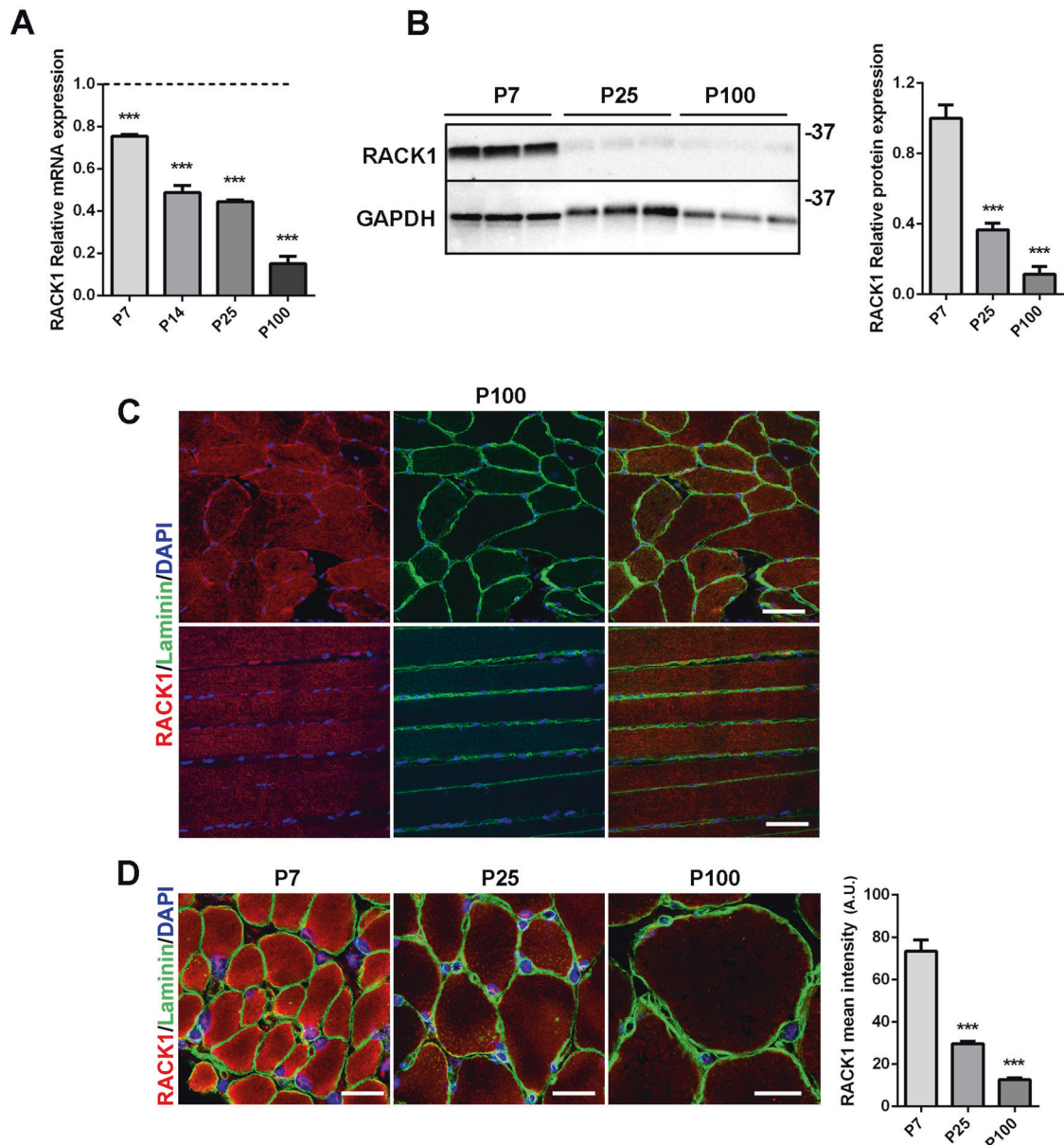


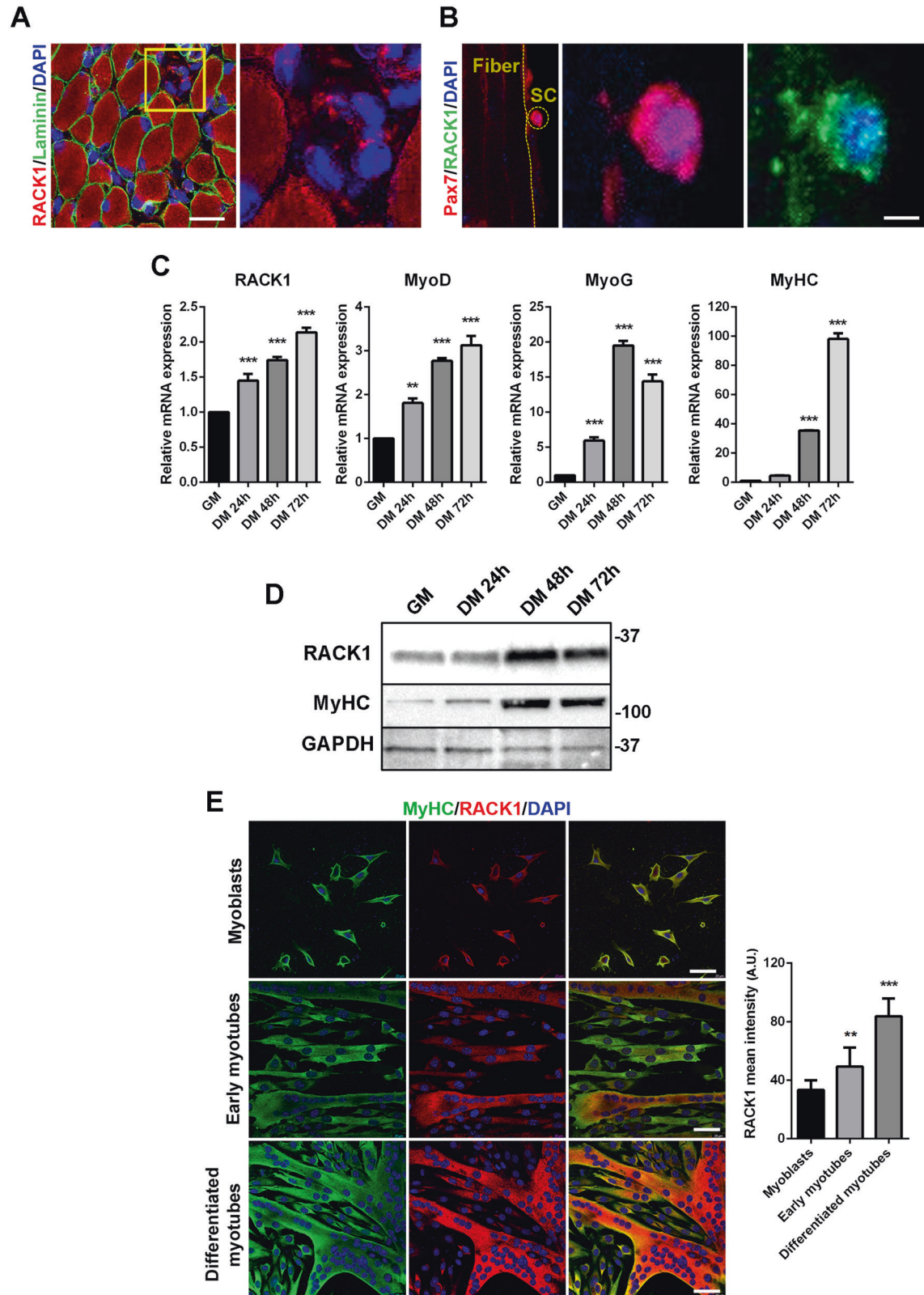
Fig. 1 RACK1 expression in postnatal mouse muscle growth. **A** mRNA levels of RACK1 by RT-qPCR in TA muscle of P0, P7, P14, P25, and P100 mice. Results are expressed as fold change of P0 (dashed line). $***P < 0.001$ vs P0 mice. **B** Western blot analysis of RACK1 in TA muscle of P7, P25, and P100 mice. GAPDH was used as internal standard. Right panel: densitometric quantification of RACK1; results are expressed as fold change of P7. $***P < 0.001$ vs P7 mice. **C** Confocal fluorescence imaging of RACK1 (red), Laminin (green), and DAPI (blue) in transversal (upper panels) and longitudinal (lower panels) TA muscle sections of P100 mice (scale bars: 40 μ m). **D** Confocal fluorescence imaging of RACK1 (red), Laminin (green), and DAPI (blue) in transversal TA muscle sections of P7, P25, and P100 mice (scale bars: 20 μ m). Right panel: mean RACK1 intensity signals (A.U.: arbitrary units). $***P < 0.001$ vs P7 mice. Images and quantitative data are representative of $6 \leq n \leq 10$ mice.

morphological regeneration after physical damage, some GFP-positive cells were progressively found around injured fibers indicating the recruitment of SC population. Immunofluorescence staining of RACK1 was faint in uninjured DLM of *Zfh1>GFP* flies although it somewhat co-localized with GFP⁺ SC (Fig. 5A). Noteworthy, a striking over-expression of RACK1 was associated with the injury, positioned around the damage and along the regenerating/differentiating fibers. Especially, RACK1 levels increased 1 day after damage and then progressively declined, appearing very low at 10 days when muscle tissue almost recovered. During the most active myogenesis program, i.e., 3–5 days, the presence of GFP⁺ cells high-expressing RACK1 was clearly detectable in the regeneration area around the wound. As shown in Fig. 5B, we found Jagged1 localized around the damaged

area of DLM of Oregon flies during the active regeneration phase. Jagged1 protein is the ortholog of the *Drosophila* Notch ligand Serrate [30, 31] and it was used here to detect active SC in flies as in mouse muscle. Noteworthy, Jagged1 staining was detected in RACK1 overexpressing injured tissue.

RACK1 depletion in SC impairs myogenic progression

To further understand the myogenic role of RACK1, we down-regulated RACK1 in mouse SC by RNA interference. Hence, SC were transfected with either a RACK1-specific or a non-targeting siRNA and cultured in GM for 24 h. PCR and western blot analysis identified a significant decrease of RACK1 transcript (Fig. 6A) and protein (Fig. 6B) of about 60%. A similar downregulation of RACK1 was maintained after 24 and 48 h of DM (Supplementary Fig. S1B),



indicating a persistent efficacy of siRNA effects during myogenic progression. As shown in Fig. 6C, D, RACK1 silencing did not seem to affect SC proliferation when compared to mock-transfected control and this is confirmed by unchanged KI-67 and cyclin D1 mRNA levels (Supplementary Fig. S1C). Subsequently, after siRNA

transfection in GM, SC were switched to DM for 48 h to examine differentiated efficiency [27]. Both control and RACK1 siRNA SC formed multinucleated myotubes although we observed defective myotube growth in the presence of low levels of RACK1 (Fig. 6E, F). In particular, the fusion index, the myotube diameter, the mean

Fig. 2 RACK1 expression in mouse SC and in deriving myotubes. **A** Confocal fluorescence imaging of RACK1 (red), Laminin (green), and DAPI (blue) in transversal TA muscle sections of P7 mice (scale bar: 20 μ m). Insert represents enlarged image details of RACK1⁺ interstitial cells showed in the right panel. Images are representative of 6 mice. **B** Confocal fluorescence imaging of Pax7 (red), RACK1 (green), and DAPI (blue) in TA-isolated fiber with enlarged image details of double RACK1⁺ and Pax7⁺ SC showed in the right panels (scale bar: 40 μ m). Images are representative of 20 $\leq n \leq 30$ experiments. **C** mRNA levels of RACK1, MyoD, MyoG, and MyHC by RT-qPCR in proliferating (GM) and differentiating (DM) SC at increasing times. Results are expressed as fold change of GM SC. **D** Western blot analysis of RACK1 and MyHC in GM and DM SC at increasing times. GAPDH was used as internal standard. **E** Confocal fluorescence imaging of RACK1 (red), MyHC (green), and DAPI (blue) in GM SC (myoblasts) and in early (24 h DM SC) and differentiated (48 h DM SC) myotubes (scale bars: 40 μ m). Right panel: mean RACK1 intensity signals (A.U.: arbitrary units). ** $P < 0.01$ and *** $P < 0.001$ vs GM SC. Images and quantitative data are representative of 8 $\leq n \leq 10$ experiments.

number of nuclei/myotube, and the number of myotubes with 5 or more nuclei were significantly lower in RACK1 siRNA versus control SC (Fig. 6G). Consistently, the expression level of the myogenic marker MyoG was significantly reduced in RACK1 siRNA SC (Fig. 6H).

RACK1 coupling to proteostasis operates on SC activation

To gain mechanistic insights, we tested whether RACK1 might regulate cellular stress response since it is a common pathway involved in SC function/dysfunctions, also interacting with catabolic systems such as autophagy [4]. After RACK1 siRNA transfection in GM, mouse SC were switched to DM for 24 h to examine different transcripts involved in muscle unfolded protein response (UPR), i.e., the activating transcription factors (ATF) 3, 4, or 6, the transcription factor C/EBP homologous protein (CHOP), and the ER chaperon GRP78/BiP [36]. As shown in Fig. 7A, RACK1 silencing significantly up-regulated the UPR markers when compared to control. To note, both the mRNA of MyoD (Fig. 7B) and its fluorescence immunostaining (Fig. 7C) were significantly reduced in SC after RACK1 silencing. In contrast, the sustained turnover of autophagy process in differentiating SC was not modified by low RACK1, since protein levels of the autophagy factors LC3/II and p62 did not change (Fig. 7D).

RACK1 is required for proper regeneration of *D. melanogaster* skeletal muscle following injury

The functional role of RACK1 was then investigated in vivo in *Drosophila* myogenesis upon physical damage. To this aim, UAS-RACK1 IR and Mef2-Gal4 flies were crossed as previously reported [24], producing F1 progeny in which the Rack IR construct became expressed following the Mef2 promoter, affecting late myogenesis, during the overt differentiation phase [37]. We thus obtained adult *D. melanogaster* phenocopies (Mef2>RACK1 IR) with silenced levels of RACK1 in muscle cells. As shown in Supplementary Fig. S2A, confocal microscopy did not reveal evident morphological changes in DLM structure. Accordingly, the climbing ability (vertical walking) of Mef2>RACK1 IR flies was not different from that observed in the presence of wild-type RACK1 (Supplementary Fig. S2B). Similar results were obtained when we compared the longevity of *Drosophila* strains (Supplementary Fig. S2C), indicating that alteration of RACK1 in adult skeletal muscle of flies does not impact on their general phenotype, locomotor ability, and lifespan.

We then tested the muscle regeneration efficiency in RACK1 silenced flies. The injury wound in DLM of Mef2>RACK1 IR young adults was still clearly evident 5–10 days after injury and regenerated phenotype manifested at 15 days, while the onset-recovery of Mef2-Gal4 controls superimposed with the wild-type strains shown before (Fig. 8A). Accordingly, the repair process (size reduction) of the wound was significantly delayed in Mef2>RACK1 IR flies (Fig. 8B). As expected, at day 5 after injury, the immunofluorescence staining of RACK1 in the damaged area of DLM was clearly reduced in Mef2>RACK1 IR when compared with Mef2-Gal4 *Drosophila* (Fig. 8C). To note, Mef2>RACK1 IR injury exhibited faint expression of Jagged1 fluorescence, i.e., active SC. In particular, Jagged1 in the damaged area of Mef2>RACK1 IR *Drosophila* significantly decreased of about 44% versus control.

These results suggest that RACK1 silencing impairs the activation of SC involved in the repair process.

To further assess whether the observed RACK1-interfered phenotypes were strictly associated to SC activity, we performed RNAi silencing of RACK1 specifically in SC crossing Zfh1-Gal4 and UAS-RACK1 IR lineage. Overall, the parameters observed with SC-specific downregulation of RACK1 in Zfh1>RACK1 IR *Drosophila*, i.e., the onset-recovery of DLM damage after physical injury (Fig. 8D, E), the immunostainings of RACK1/Jagged1, and the Jagged1 quantification at day 5 after injury (Fig. 8F), were superimposable with those seen in Mef2>RACK1 IR flies.

Finally, we took advantage of RACK1 silencing in SC of flies to test the involvement of ATF in RACK1-induced SC activation, since the UPR pathways are common between *Drosophila* and humans [38]. In particular, the *Drosophila* genome has a conserved ATF4 gene, also referred to as cryptocephal. As shown in Fig. 8G, the immunofluorescence staining of ATF4 in the damaged area of DLM at day 5 after injury was clearly overexpressed in Zfh1>RACK1 IR when compared with Zfh1-Gal4 *Drosophila*.

DISCUSSION

RACK1 has been previously associated to cell growth/proliferation and survival [7, 8, 16, 19]. For instance, neural development seems to require RACK1 [39, 40]. Thus, it is not surprising that RACK1 was expressed transiently in the skeletal muscle of post-natal mice, being abundant in the early phase of muscle growth and almost disappearing in adult mature fibers. When muscle develops SC proliferate and differentiate actively to form new fibers before entering a quiescent state. Pax7 is a pivotal regulator of SC specification [4–6]. The presence of RACK1 in interstitial Pax7⁺ SC tissue prompted us to hypothesize that RACK1 is important for skeletal muscle growth.

Once activated SC support growth and regeneration [3–6]. The dynamics of RACK1 levels in isolated adult SC of mice, progressively high during differentiation and low compared to proliferating conditions, suggested that RACK1 activity could be required for the myogenic program of SC, i.e., in nascent myotubes which are progressing towards mature differentiation. In adult skeletal muscle, the majority of SC are quiescent, but are poised for activation/differentiation in response to exercise, injury, or disease [3–6]. After muscle injury we found that RACK1 accumulated in mouse regenerating fibers during the remodeling phase, while it declined with the progression of regeneration. Consistent with these results, RACK1 accumulated in peripheral Jagged1⁺ cells, likely interstitial active SC that populate regenerating tissue. Indeed, Notch signaling, including Jagged1, is crucial in postnatal myogenesis for SC functions [30, 31]. Accordingly, Jagged1 expression was upregulated in regenerating fibers of mice after CTX-induced injury and during myoblast muscle differentiation in vitro [41]. Notwithstanding numerous differences in the growth of vertebrate and *Drosophila* muscles, there are remarkable similarities in the fundamental myogenic processes [42, 43]. For instance, SC are available for adult myogenesis in flies in response to damage, thus highlighting *Drosophila* as a model to understand muscle homeostasis [33, 43]. In addition, both the

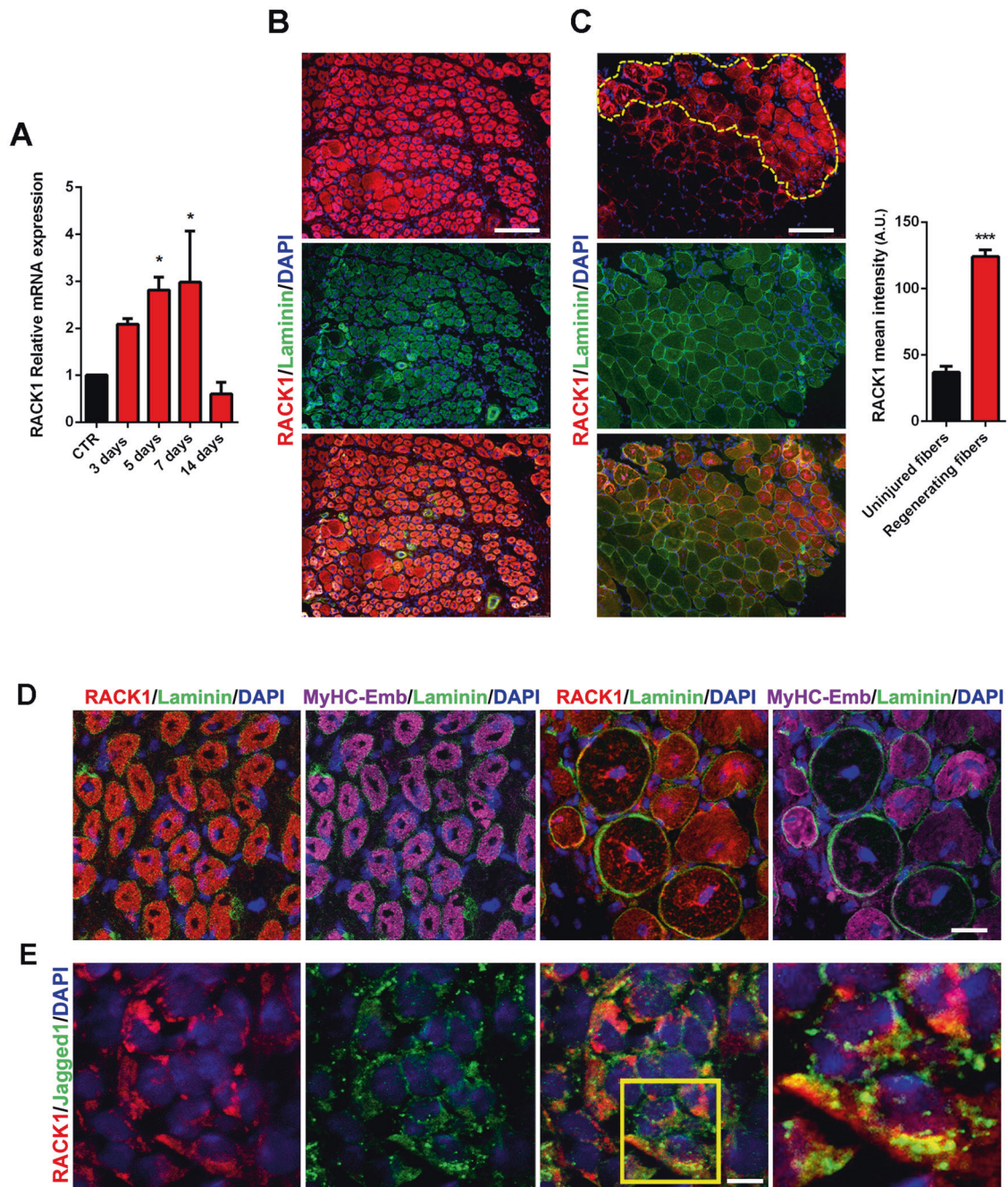


Fig. 3 RACK1 expression in response to mouse muscle acute damage. **A** mRNA levels of RACK1 by RT-qPCR in TA muscle of CTX-injected mice at 3, 5, 7, and 14 days. Results are expressed as fold change of control (CTR, not injected) muscle (dashed line). Data are representative of 4 mice. * $P < 0.05$ vs CTR. **B, C** Confocal fluorescence imaging of RACK1 (red), Laminin (green), and DAPI (blue) in transversal TA muscle sections after 7 days post CTX injection (scale bars: 50 μm). The dashed yellow line represents the regenerating area. Right panel: mean RACK1 intensity signals in regenerating compared to uninjured fibers (A.U.: arbitrary units). *** $P < 0.001$ vs uninjured. **D** Confocal fluorescence imaging of RACK1 (red), Laminin (green), MyHC-Emb (purple), and DAPI (blue) in transversal TA muscle sections after 7 days post CTX injection (scale bar: 20 μm). **E** Confocal fluorescence imaging of RACK1 (red), Jagged1 (green), and DAPI (blue) of interstitial activated SC in transversal TA muscle sections at 7 days after CTX injection (scale bar: 5 μm). Insert represents enlarged image details of RACK1⁺/Jagged1⁺ cells showed in the right panel. Images and quantitative data are representative of 6 mice.

human and *Drosophila* genomes encode a single RACK1 gene and alignment of RACK1 protein sequence reveals strong conservation [44]. Thus, as alternative valuable *in vivo* tool, we set-up a *Drosophila* model with induced physical damage in skeletal muscles. As previously published in different fly strains [32], physical injury almost completely recovered after damage. Despite RACK1 being scarcely detected in intact or recovered fibers, it transiently increased in the wound area as a quick event during

the repair process. RACK1 localized in the regenerating/differentiating fibers around the damage and in some *zfh1*-expressing SC. It was demonstrated that the activation of the normally quiescent *zfh1* lineage anticipates the fusion with the damaged fibers in muscle repair, and that *zfh1* was then down-regulated during the quiescent-active transition [32]. Our results were thus consistent with the role of RACK1 in the early phase, during which SC are committed to fuse and differentiate. Similar to mice, the

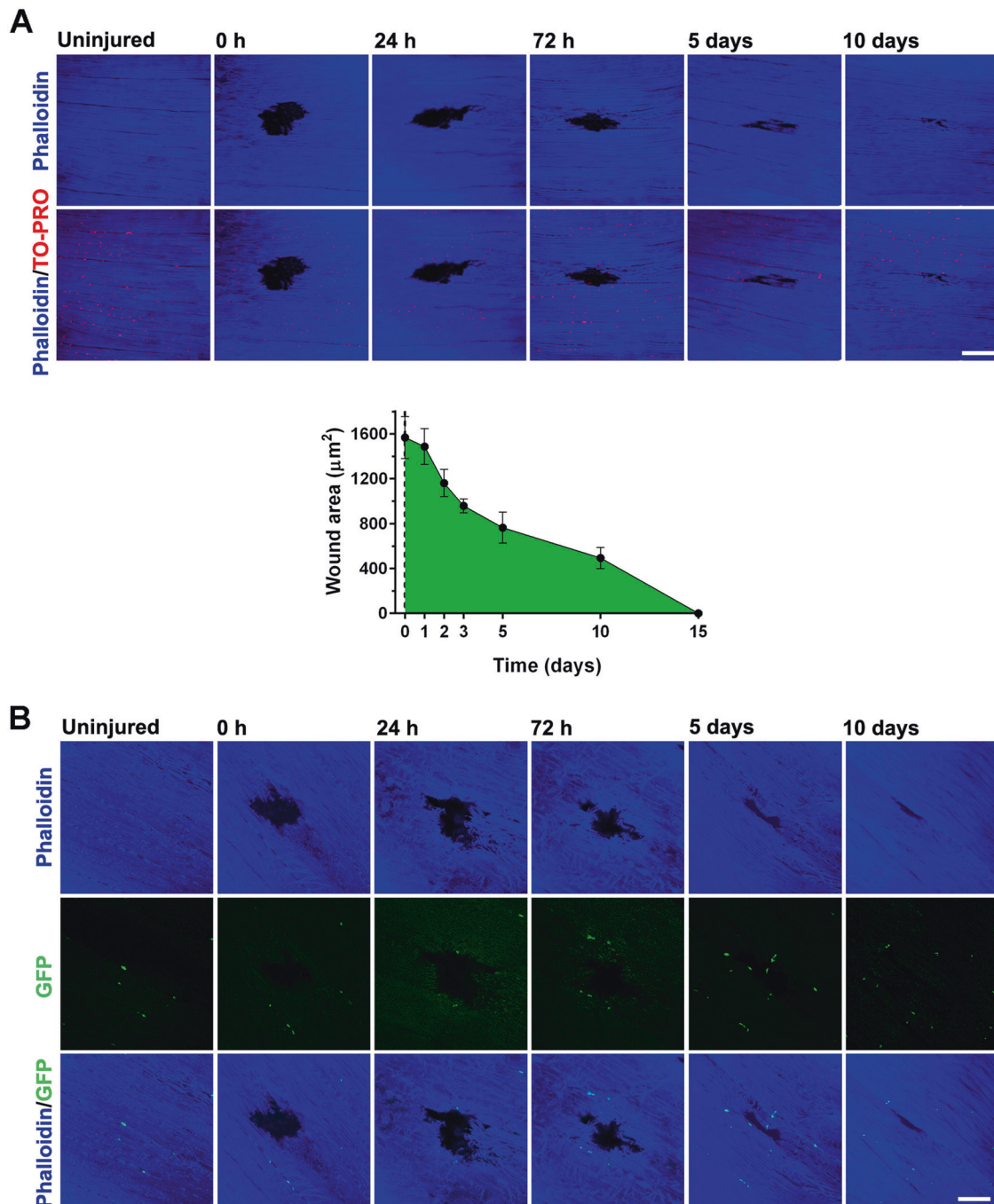


Fig. 4 Acute skeletal muscle injury in *D. melanogaster*. **A** Confocal fluorescence imaging of Phalloidin (blue) and TO-PRO (red) in DLM longitudinal sections of Oregon wild-type fly strain before (uninjured) and after physical damage at increasing times. Low panel: time-course measurement of the wound area. **B** Confocal fluorescence imaging of Phalloidin (blue) and GFP (green) in DLM longitudinal sections of *Zfh1>GFP* flies before (uninjured) and after physical damage at increasing times. Scale bars: 20 µm. Images and quantitative data are representative of $30 \leq n \leq 60$ flies.

possibility that active SC expressed high levels of RACK1 was confirmed by Jagged1 staining. Notch signaling is markedly conserved from *Drosophila* to humans, being the *Drosophila* protein Serrate the ortholog of the vertebrate protein Jagged1 [30, 31]. Following muscle injury in flies, SC undergo symmetric divisions through Notch signaling, that is also necessary for maintaining *zfh1* expression [35]. Taken together these results indicated that RACK1 is a novel well conserved factor of SC whose expression mirrors SC activation and is closely associated with muscle growth/regeneration.

While inactivation of RACK1 was devoid of effects on adult SC proliferation, here we describe how RACK1-depleted SC were impaired in the differentiation process. Differentiation of SC occurs in 2 phases: single myoblasts fuse to form nascent myotubes, followed by recruitment of new nuclei to existing myotubes, leading to larger fully differentiated, multinucleated myotubes. The fusion index is a valid proxy of the first phase efficiency, while the mean number of nuclei/myotube and the percentage of myotubes with 5 or more nuclei are indexes of second phase effectiveness [27]. Our results in isolated mouse SC demonstrated

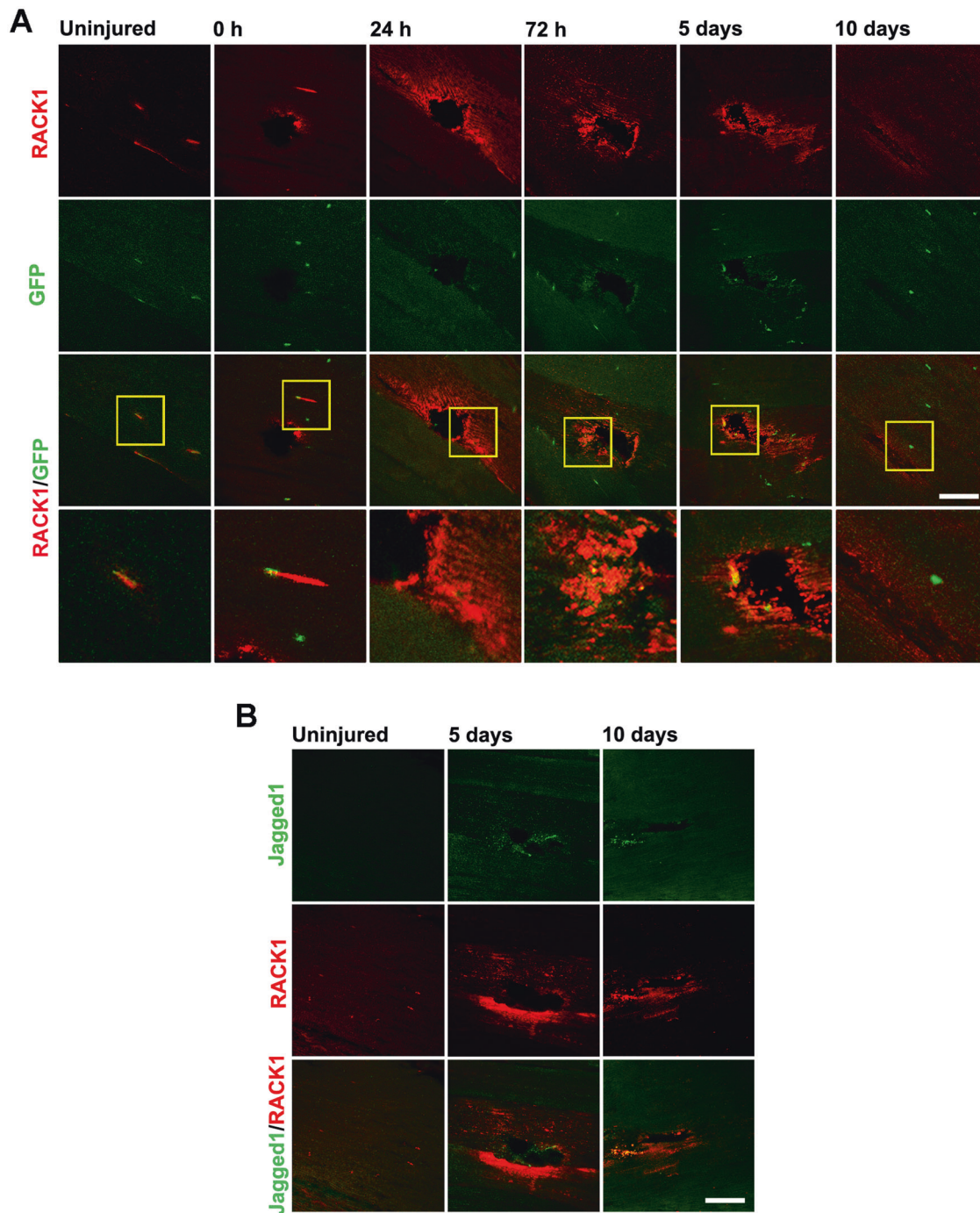
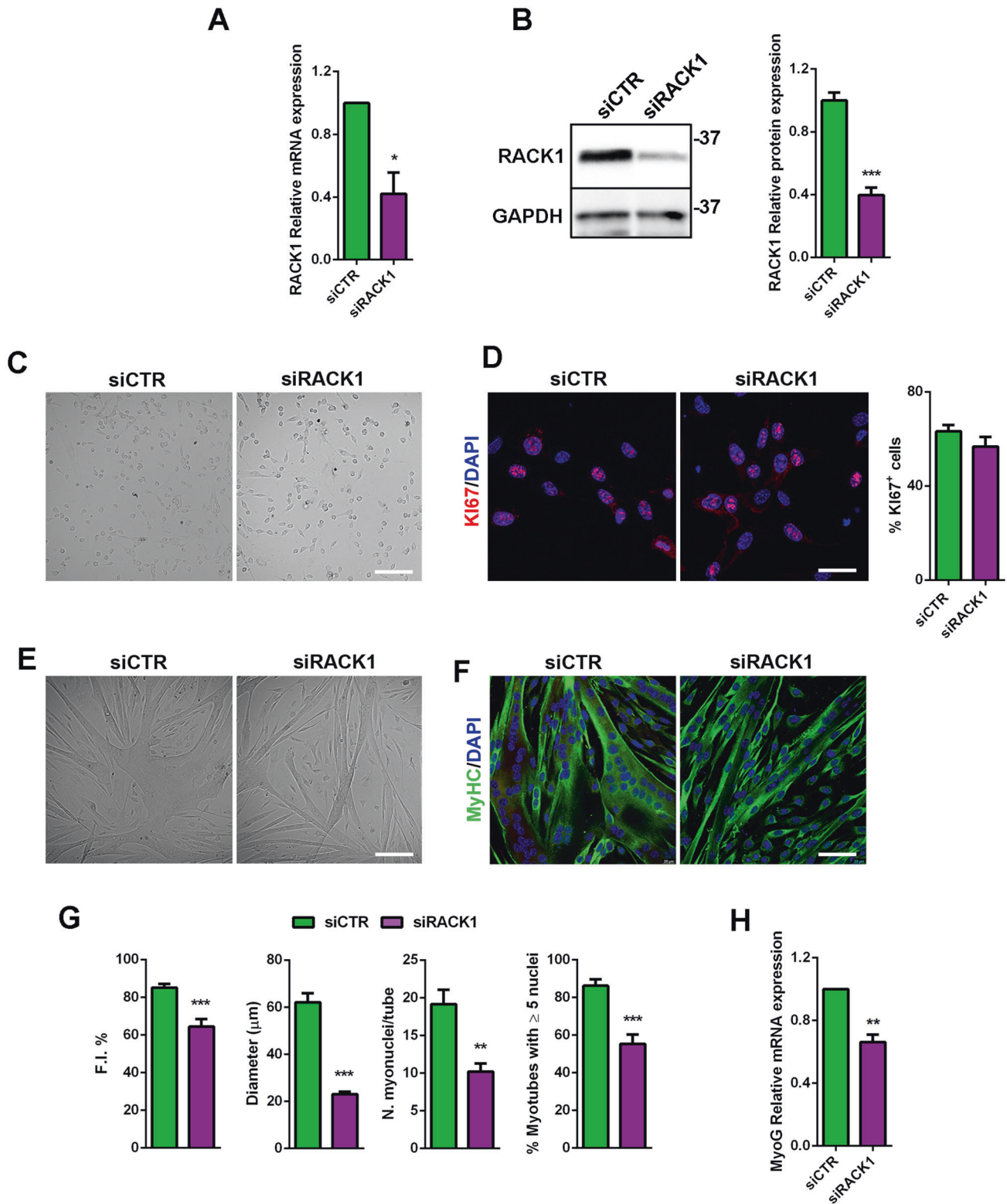


Fig. 5 RACK1 expression in response to *D. melanogaster* muscle acute injury. **A** Confocal fluorescence imaging of RACK1 (red) and GFP (green) in DLM longitudinal sections of *Zfh1>GFP* flies before (uninjured) and after physical damage at increasing times. Inserts represent enlarged image details showed in the low panels. Images are representative of $30 \leq n \leq 40$ flies. **B** Confocal fluorescence imaging of Jagged1 (green) and RACK1 (red) in DLM longitudinal sections before (uninjured) and after physical damage at increasing times. Scale bars: 20 μ m. Images are representative of $15 \leq n \leq 20$ flies.

that RACK1 promotes both the formation of myotubes and the accretion of nascent myotubes. Interestingly, in the presence of low RACK1, SC somewhat formed multinucleated myotubes although they cannot ultimate the differentiation program efficiently, as also suggested by the downregulation of MyoD and MyoG, early and late differentiation markers, respectively [4–6, 28]. Impaired differentiation ability of in vitro SC with defective RACK1 is consistent with the regenerative response obtained in vivo in *Drosophila* with depleted RACK1. Relevant to

this study, homozygous knockout of RACK1 is lethal in mice [45]. In addition, the genetic handling of muscle cells may lead to death in rodents but not in *Drosophila* muscles [46, 47]. In both *Mef2>RACK1* IR and *Zfh1>RACK1* IR flies, in which RACK1 gene was silenced in all muscle cells (both progenitors and differentiated cells of the somatic muscle) or, specifically, in SC lineage, respectively, we observed a significant and similar delayed recovery of skeletal muscle after physical damage. Additionally, the low expression of RACK1 in the wound regenerative area



significantly reduced Jagged1⁺ staining (active SC), further demonstrating the role of RACK1 in promoting SC activation and inducing efficient myogenesis.

The UPR is a conserved protein handling network that promotes the elimination of misfolded proteins and plays an important role in the survival, self-renewal, and differentiation of stem cells. It may regulate the SC transition to the activated state both in vitro and

in vivo, also by interacting with catabolic systems such as autophagy [4, 36]. UPR and autophagy pathways play pivotal roles in regeneration of injured skeletal muscle [4, 36, 48]. While autophagy mechanisms in isolated mouse SC were not affected by RACK1 depletion, we observed increased levels of ATF3, 4, and 6 as well as CHOP and GRP78/BiP, thus indicating that RACK1-induced differentiation may involve, at least in part, the inhibition of UPR

Fig. 6 RACK1 downregulation affects mouse SC differentiation. Proliferating (GM) SC were transfected for 24 h with a RACK1-specific (siRACK1) or a non-targeting siRNA (siCTR). **A** mRNA levels of RACK1 by RT-qPCR. Results are expressed as fold change of siCTR. **B** Western blot analysis of RACK1. GAPDH was used as internal standard. Right panel: densitometric quantification of RACK1; results are expressed as fold change of siCTR. **C** Bright-field images (scale bar: 100 μ m). **D** Confocal fluorescence imaging of Ki67 (red) and DAPI (blue) (scale bar: 40 μ m). Right panel: percentage of Ki67⁺ cells on total DAPI-stained nuclei. SC were transfected for 24 h in GM with a RACK1-specific (siRACK1) or a non-targeting siRNA (siCTR), and then cultured for 48 h in differentiating (DM) conditions. **E** Bright-field images (scale bar: 100 μ m). **F** Confocal fluorescence imaging of MyHC (green) and DAPI (blue) of forming myotubes (scale bar: 40 μ m). **G** Fusion index (F.I.), mean myotubes diameter, mean number of myonuclei/myotube, and percentage of myotubes with 5 or more nuclei. **H** mRNA levels of MyoG by RT-qPCR. Results are expressed as fold change of siCTR. * $P < 0.05$, ** $P < 0.01$, and *** $P < 0.001$ vs siCTR. Images and quantitative data are representative of $6 \leq n \leq 8$ experiments.

genes. In support of this hypothesis, we found that impaired levels of RACK1 in *Drosophila* SC induced ATF4 overexpression around the injury of regenerating muscles. As in other organisms, the stress response was shown to increase *Drosophila* ATF4 [49, 50]. To notice, our results suggest the evolutionary conservation of RACK1 and UPR coupling during SC activation. The increased levels of UPR signals may inhibit SC through repressing MyoD and in turn myogenesis [36, 51]. Accordingly, RACK1 silencing in isolated mouse SC inhibited MyoD. In multiple systems, RACK1 acts as a ribosomal scaffolding protein, modulating the translation of mRNAs and polypeptide synthesis, thus providing a hub integrating cell signaling and global protein [8, 13, 16, 17]. In this respect, RACK1 regulates myoproteostasis of *Drosophila* aging muscle, since it contributes to the modulation of misfolded protein aggregates, locomotor function, and longevity through the regulation of protein synthesis [24].

Collectively, in our study we found that RACK1 is mostly expressed in active SC and regenerating fibers respect to mature skeletal muscle cells, indicating that RACK1 is important for SC function. Specifically, we provide the first evidence that transient levels of RACK1 in SC are critical for efficient myogenesis to occur both in vitro and in vivo. Indeed, RACK1 favors the efficient progression of SC from a committed to a fully differentiated state, likely acting, at least in part, on UPR pathway. In this line, we demonstrated that RACK1 guarantees a proper SC-induced repair process in adult skeletal muscle after acute injury, while RACK1 defects determine delayed myogenesis and recover. Our findings highlight how the evolutionarily conserved RACK1 system deserves to be further investigated to achieve information translationally suited in muscle degenerative disorders and during aging.

MATERIALS AND METHODS

Chemicals

Phosphate buffer saline (PBS), Dulbecco's Modified Eagle Medium (DMEM), penicillin-streptomycin, fetal bovine serum (FBS), and Horse serum (HS) were purchased from EuroClone (Pero, Italy). Chick embryo extract was obtained from United States Biological (Salem, MA, USA). Basic fibroblast growth factor (FGFb) was purchased from PeproTech (Cranbury, NJ, USA). The primary antibodies, including their suppliers, are listed in Supplementary Table S1. The primers pairs (Supplementary Table S2) were purchased from Eurofins (Vimodrone, Italy). The cocktail of protease and phosphatase inhibitors cComplete and PhosSTOP was obtained from Roche Applied Science (Mannheim, Germany). Horseradish-peroxidase-conjugated secondary antibodies were purchased from Cell Signaling Technology (Danvers, MA, USA). Fluoroshield Mounting Medium containing DAPI and fluorescent phalloidin (#ab176752) were obtained from Abcam (Cambridge, UK). DAPI, Alexa-conjugates and TO-PRO™-3 Iodide (#T3605) were purchased from Invitrogen-ThermoFisher Scientific (Waltham, MA USA). Normal goat serum was obtained from Vector Laboratories (Newark, CA, USA). All other chemicals were from Sigma-Aldrich Merck (Darmstadt, Germany).

Mice

C57BL/6 mice were purchased from Charles River Laboratories (Calco, Italy), housed in a regulated pathogen-free environment (23 ± 1 °C, $50 \pm 5\%$ humidity) with a 12 h light/dark cycle (lights on at 08.00 a.m.), and provided with food and water ad libitum. When indicated, both male and

female mice were euthanized at different ages. Procedures were carried out in strict accordance with the Italian law on animal care (D.L. 26/2014, implementation of the 2010/63/UE) and approved by University of Milan Animal Welfare Body and by the Italian Minister of Health.

D. melanogaster strains and husbandry

Wild-type (Oregon-R strain) and transgenic flies were obtained from Bloomington *Drosophila* Stock Center (BDSC, Indiana University Bloomington, IN, USA). As previously reported [52, 53], flies were routinely raised on a corn meal agar food (pH 5.5) at 25 °C, following standard mating procedures.

The fly strain *Dmel\{ET1\}zfh1^{MB07519}* (BDSC#25351; abbreviated as Zfh1-Gal4), which carries Gal4 insertion in the zfh1 locus, was crossed with UAS-mCD8::GFP flies (BDSC#5137) to obtain Zfh1>GFP progeny. In addition, flies expressing dsRNAi of RACK1 under UAS control (UAS-RACK1 IR; BDSC#38198) were crossed with flies expressing Gal4 under the control of the specific muscle driver DMef2 (Mef2-Gal4; BDSC#26882 and BDSC#27390) or with Zfh1-Gal4 flies. The F1 progeny obtained from these crosses (Mef2>RACK1 IR and Zfh1>RACK1 IR) was, at least in part, viable thus suggesting that the attenuation of RACK1 in muscles of flies does not induce drastic premature lethality.

Primary mouse SC isolation and culture

As previously published [27, 54, 55], primary cultures of SC from 25 days old mice were obtained from dissociated muscles of hindlimbs and forelimbs by using the tissue dissociation protocol of gentleMACS™ Octo Dissociator with Heaters (Miltenyi Biotec, Bergisch Gladbach, Germany) followed by magnetic depletion of lineage ITGAM/CD11b (integrin alpha M), PECAM1/CD31 (platelet/endothelial cell adhesion molecule 1), PTPRC/CD45 (protein tyrosine phosphatase, receptor type, C) and LY6A/Sca-1 (lymphocyte antigen 6 complex, locus A) to exclude the Lin-negative population, using the Satellite Cell Isolation Kit (Miltenyi Biotec), according to the manufacturer's protocols. SC were cultured in DMEM supplemented with 20% FBS, 3% chick embryo extract, 10 ng/mL FGFb and 1% penicillin-streptomycin on matrigel-coated plates at 37 °C with 5% CO₂ for 4 days. To assess proliferation, SC were plated at a confluence of 1.5×10^4 cell/cm² in GM and cultured for 24 h. For the differentiation experiment, cells were plated at a confluence 5×10^4 cell/cm² in DM containing 2% HS instead of FBS and cultured for 24–72 h.

RNA interference

According to the manufacturer's protocol, RACK1 siRNA pool of 3 target-specific mouse Rack1 (Santa Cruz Biotechnology, Dallas, TX, USA) were mixed to Lipofectamine RNAiMax transfection reagent (Invitrogen-ThermoFisher Scientific). Control non-targeting siRNAs siRNA negative control (Santa Cruz Biotechnology) were also used. The mix was added to SC cells cultured in GM at a siRNA concentration of 10–50 nM for 24 h.

Models of skeletal muscle injury

Acute muscle damage in mice was induced by injection of CTX from *Naja pallida* (50 μ L, 10 μ M) in TA muscle of 6–8 weeks old anesthetized mice, as previously described [56]. Mice were sacrificed 3, 5, 7, and 14 days after injury before muscle collection.

Fly muscle injury was performed as previously described [32, 57] with minor changes. Briefly, young-adults (2–3 days of adult age) flies were anesthetized with triethylamine and placed laterally under a stereo microscope. Only one of the two hemithorax was manually injured at DLM by inserting a thin pin (Minutien Pins-Stainless Steel/0.1 mm diameter #26002–10, Fine Science Tools, Heidelberg, Germany) for approximately

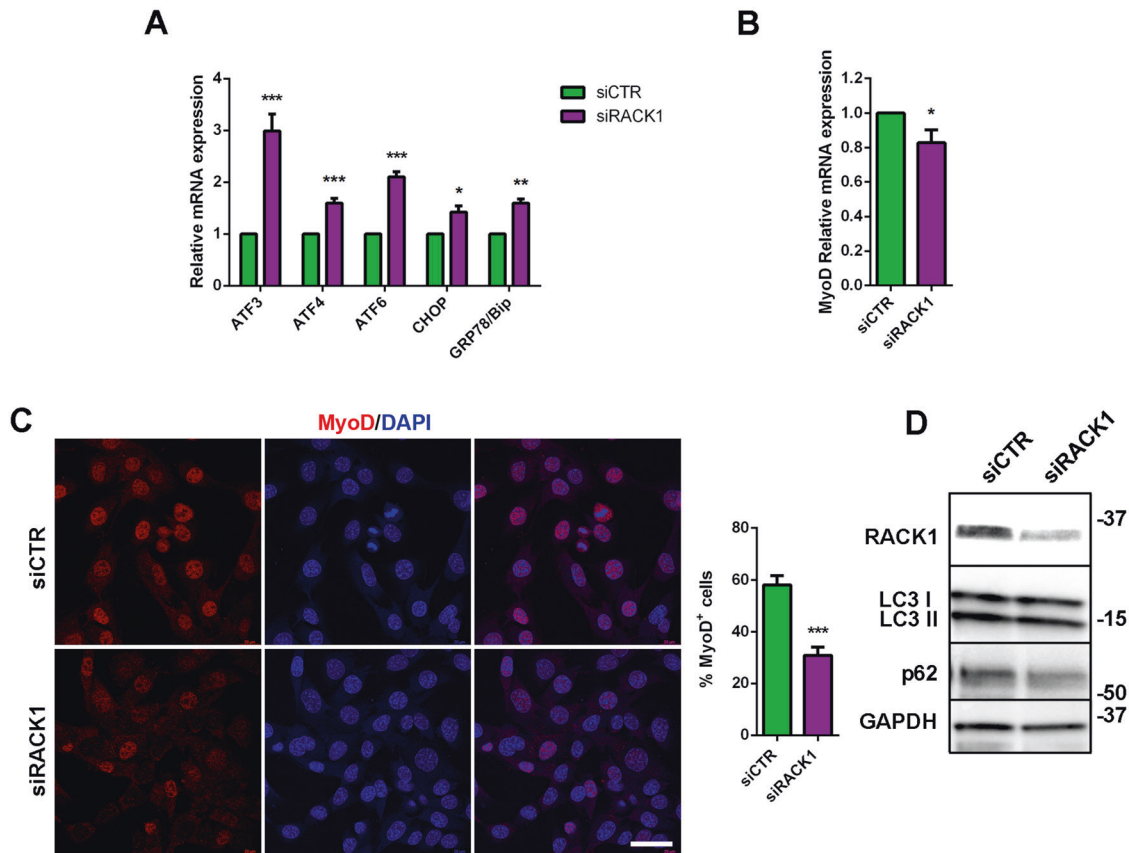


Fig. 7 RACK1 downregulation in mouse SC is associated to UPR response. SC were transfected for 24 h in proliferating (GM) conditions with a RACK1-specific (siRACK1) or a non-targeting siRNA (siCTR), and then cultured for 24 h in differentiating (DM) conditions. **A**, **B** mRNA levels of UPR genes (ATF3, 4, 6, CHOP, and GRP78/Bip) and MyoD by RT-qPCR. Results are expressed as fold change of siCTR. **C** Confocal fluorescence imaging of MyoD (red) and DAPI (blue) (scale bar: 40 μ m). Right panel: percentage of MyoD⁺ cells on total DAPI-stained nuclei. **D** Western blot analysis of RACK1, LC3I/II, and p62. GAPDH was used as internal standard. * $P < 0.01$, ** $P < 0.01$, and *** $P < 0.001$ vs siCTR. Images and quantitative data are representative of $6 \leq n \leq 10$ experiments.

0.5 mm, avoiding extensive injury. Flies were recovered on standard food at 0–24–72 h and 5–10–15 days after injury before DLM collection.

RNA extraction and RT-qPCR

The analysis of mRNA expression in TA muscle and SC of mouse was performed in PureZOL reagent (Bio-Rad, Hercules, CA, USA). Total RNA (500–800 μ g) was retro-transcribed using iScript gDNA Clear cDNA Synthesis Kit (Bio-Rad). RT-qPCR was performed using SsoAdvanced™ Universal SYBR Green Supermix (Bio-Rad) and the CFX96 Touch Real-Time PCR Detection System (Bio-Rad). The primers pairs designed for RT-qPCR are detailed in Supplementary Table S2. Rpl38 and 36B4 have been used as housekeeping genes for normalization by using the $2^{-\Delta\Delta CT}$ method.

Western blot

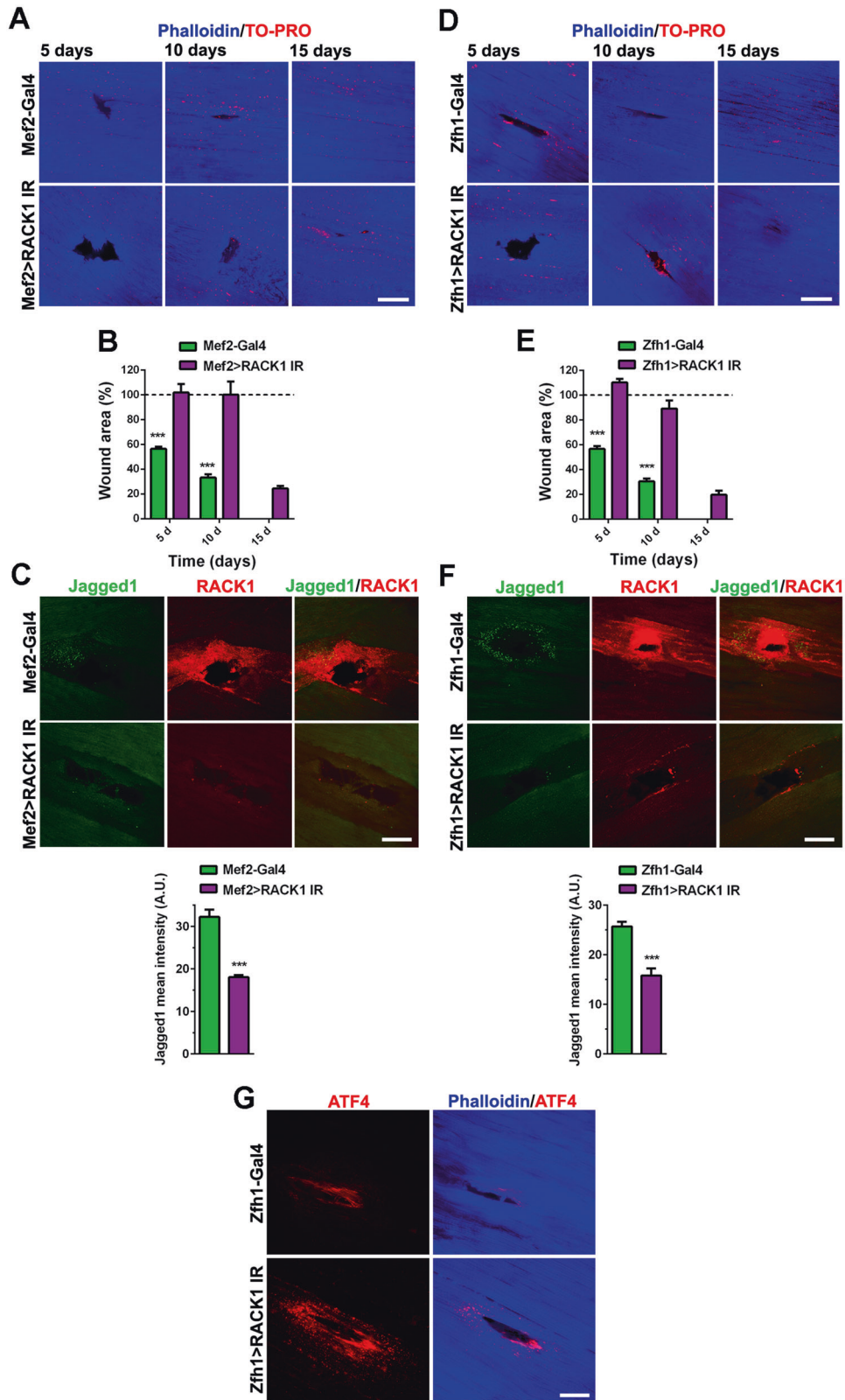
TA muscles were homogenized with Ultra-Turrax (Ika Werke, Staufen, Germany) in a lysis buffer containing 20 mM Tris-HCl (pH 7.4), 10 mM EGTA, 150 mM NaCl, 1% Triton X-100, 10% glycerol, 1% Sodium Dodecyl Sulfate (SDS) supplemented with protease and phosphatase inhibitors. Protein extracts from cells were performed in RIPA buffer (10 mM Tris-Cl (pH 8.0), 140 mM NaCl, 1 mM EDTA, 0.5 mM EGTA, 1% Triton X-100, 0.1% sodium deoxycholate, 0.1% SDS) supplemented with protease and phosphatase inhibitors. Proteins were quantified using a BCA protein assay kit (Pierce, Rockford, IL, USA) following the standard protocol for western blotting. Thirty to fifty μ g of total protein were loaded on 4–20% polyacrylamide precast gels (Criterion TGX Stain-free precast gels; Bio-Rad). Proteins were transferred onto a nitrocellulose membrane using a Trans-Blot Turbo System™ (7 min at 2.5 A) and Transfer pack™ (Bio-Rad). Primary antibodies used to probe membranes are indicated in Supplementary Table S1. After the incubation with the appropriate horseradish-peroxidase-conjugated secondary antibody [58], bands were visualized

using the Clarity Western ECL substrate with a ChemiDoc MP imaging system (Bio-Rad). Bands were quantified for densitometry using the Bio-Rad Image Lab software. Uncropped western blots are provided in Supplementary Material.

Fluorescence microscopy

For immunofluorescence experiments in TA muscle/single fiber and SC of mouse we followed a standard protocol [27, 59, 60]: samples were fixed with Paraformaldehyde (PFA) 4% for 10 min and permeabilized with 0.1% TritonX-100 in PBS 5 min, then blocked for 1 h in blocking buffer containing 5% normal goat serum and PBS. All primary antibodies (Supplementary Table S1) were diluted in blocking buffer and incubated overnight at 4°C. Samples were washed three times with PBS and incubated with fluorophore-conjugate (Alexa-conjugates) secondary antibodies for 1 h at room temperature and nuclei were counterstained with DAPI (1:1000), for nuclei detection. Slides were mounted with Fluoreshield Mounting medium. Single myofibers were obtained from isolated TA muscles after 4% PFA fixation (1 h at room temperature): myofibers were dissected under a stereomicroscope and collected in PBS, then stained following the standard immunofluorescent protocol. Confocal images were acquired on a TCS SP8 System equipped with a DMI8 inverted microscope and a HC PL APO 40x/1.30 Oil CS2 (Leica Microsystems, Wetzlar, Germany) at a resolution of 1024 \times 1024 pixels (single stack).

Drosophila thoraxes were collected and immersion-fixed for 2 h in cold 4% paraformaldehyde in 0.1 M Phosphate Buffer (PB) at 4°C. Samples were then transferred to cold 20% sucrose in PB and stored at 4°C for at least 24 h. Longitudinal sections of DLM (20 μ m) were obtained by a cryostat, mounted onto positive charged slides, and stored at –20°C until use. For immunostaining detection, sections were washed in PB and then pre-incubated for 1 h at room temperature with 5% BSA and 10% of normal goat serum in PB containing 0.5% Triton X-100. Pre-treated sections were



incubated for 48 h at 4°C with the primary antibodies listed in Supplementary Table S1 in PB containing 0.5% Triton X-100. GFP antibody was used to enhance the signal of fluorescent SC in Zfh1>GFP flies. Following washes in PB, the sections were incubated in the appropriate fluorophore-conjugate (Alexa-conjugates) secondary antibodies in PB overnight at room temperature. Images were acquired by a LSM 710

confocal microscope and a Plan-Apochromat 63×/1.40 Oil DIC M27 or EC Plan-Neofluar 40×/1.30 Oil DIC M27 (Carl Zeiss, Oberkochen, Germany) at a resolution of 1024 × 1024 pixels. The distance between adjacent focal planes (z-stacks) was set at 1 μm. Fluorescent phalloidin (F-actin staining, 1:1000) was used to observe *Drosophila* muscle structure and TO-PRO™-3 iodide (1:1000) for nuclei detection.

Fig. 8 RACK1 downregulation affects *D. melanogaster* muscle regeneration. **A, D** Confocal fluorescence imaging of Phalloidin (blue) or TO-PRO (red) in DLM longitudinal sections of Mef2-Gal4/Zfh1-Gal4 (controls) and Mef2>RACK1 IR/Zfh1>RACK1 IR flies after physical damage at increasing times, and **B, E** time-course measurement of the wound area. Results are expressed as percentage of the wound area of the respective strain measured just after damage ($t = 0$ h, dotted line). **** $P < 0.0001$ vs Mef2>RACK1 IR/Zfh1>RACK1 IR. Images and quantitative data are representative of $20 \leq n \leq 30$ flies. **C, F** Confocal fluorescence imaging of Jagged1 (green) and RACK1 (red) in DLM longitudinal sections of Mef2-Gal4/Zfh1-Gal4 (controls) and Mef2>RACK1 IR/Zfh1>RACK1 IR flies 5 days after physical damage. Lower panels: mean Jagged1 intensity signals (A.U.: arbitrary units) around the injury. *** $P < 0.001$ vs the respective control. Images are representative of $10 \leq n \leq 15$ flies. **G** Confocal fluorescence imaging of ATF4 (red) and Phalloidin (blue) in DLM longitudinal sections of Zfh1-Gal4 (controls) and Zfh1>RACK1 IR flies 5 days after physical damage. Images are representative of 10 flies. Scale bars: 20 μ m.

Incubation in secondary antibodies alone was routinely performed as a negative control. When indicated, images has been analyzed by ImageJ software (National Institutes of Health, Bethesda, MD, USA).

Climbing assay and survival of *D. melanogaster*

Geotaxis was assessed using a climbing assay (negative geotaxis reflex in opposition to the Earth's gravity) as previously published with minor modifications [61]. Climbing performance was assessed at day 2–3 of adult age (just after eclosion). Survivorship was documented throughout the adult life of the flies ending at 35 days. The numbers of dead flies per vial was recorded every 7 days.

Statistics

Generally, sample size calculation was conceptualized with 5% alpha error, 80% power and appropriate effect strength. Samples were only excluded from analyses due to technical problems, e.g., pipetting error, loss/spill of samples, or defects in materials/hardware. F-test was performed to evaluate the homogeneity of variance and Shapiro-Wilk test was used for evaluating data normality. The statistical significance of raw data between the groups (completely randomized) in each experiment was evaluated using unpaired Student's *t*/Mann-Whitney tests (single comparisons) or one-way ANOVA followed by the Tukey post-test (multiple comparisons). A *p*-value ≤ 0.05 is considered statistically significant. Data belonging from different experiments (at least 4 biological replicates, *n*) were represented and averaged in the same graph. The GraphPad Prism software package (GraphPad Software, San Diego, CA, USA) was used. The results were expressed as means \pm SEM of the indicated *n* values.

DATA AVAILABILITY

The data analyzed during this study are included in this published article and the supplemental data files. Additional supporting data are available from the corresponding authors upon reasonable request.

REFERENCES

- Roman W, Pinheiro H, Pimentel MR, Segales J, Oliveira LM, Garcia-Dominguez E, et al. Muscle repair after physiological damage relies on nuclear migration for cellular reconstruction. *Science*. 2021;374:355–9.
- Roman W, Munoz-Canoves P. Muscle is a stage, and cells and factors are merely players. *Trends Cell Biol*. 2022;32:835–40.
- Charge SB, Rudnicki MA. Cellular and molecular regulation of muscle regeneration. *Physiol Rev*. 2004;84:209–38.
- Sousa-Victor P, Garcia-Prat L, Munoz-Canoves P. Control of satellite cell function in muscle regeneration and its disruption in ageing. *Nat Rev Mol Cell Biol*. 2022;23:204–26.
- Forcina L, Miano C, Pelosi L, Musaro A. An overview about the biology of skeletal muscle satellite cells. *Curr Genomics*. 2019;20:24–37.
- Schmidt M, Schuler SC, Huttner SS, von Eyss B, von Maltzahn J. Adult stem cells at work: Regenerating skeletal muscle. *Cell Mol Life Sci*. 2019;76:2559–70.
- Adams DR, Ron D, Kiely PA. Rack1, a multifaceted scaffolding protein: Structure and function. *Cell Commun Signal*. 2011;9:22.
- Nielsen MH, Flygaard RK, Jenner LB. Structural analysis of ribosomal rack1 and its role in translational control. *Cell Signal*. 2017;35:272–81.
- Ron D, Chen CH, Caldwell J, Jamieson L, Orr E, Mochly-Rosen D. Cloning of an intracellular receptor for protein kinase c: A homolog of the beta subunit of g proteins. *Proc Natl Acad Sci USA*. 1994;91:839–43.
- Mochly-Rosen D, Smith BL, Chen CH, Disatnik MH, Ron D. Interaction of protein kinase c with rack1, a receptor for activated c-kinase: A role in beta protein kinase c mediated signal transduction. *Biochem Soc Trans*. 1995;23:596–600.

- Skop AR, Liu H, Yates J 3rd, Meyer BJ, Heald R. Dissection of the mammalian midbody proteome reveals conserved cytokinesis mechanisms. *Science*. 2004;305:61–6.
- Massip L, Garand C, Labbe A, Perreault E, Turaga RV, Bohr VA, et al. Depletion of wrn protein causes rack1 to activate several protein kinase c isoforms. *Oncogene*. 2010;29:1486–97.
- Ceci M, Welshhans K, Ciotti MT, Brandi R, Parisi C, Paoletti F, et al. Rack1 is a ribosome scaffold protein for beta-actin mrna/zbp1 complex. *PLoS One*. 2012;7:e35034.
- Ceci M, Gaviraghi C, Gorrini C, Sala LA, Offenhauser N, Marchisio PC, et al. Release of eif6 (p27bbp) from the 60s subunit allows 80s ribosome assembly. *Nature*. 2003;426:579–84.
- Nilsson J, Sengupta J, Frank J, Nissen P. Regulation of eukaryotic translation by the rack1 protein: A platform for signalling molecules on the ribosome. *EMBO Rep*. 2004;5:1137–41.
- Ceci M, Fazi F, Romano N. The role of rna-binding and ribosomal proteins as specific rna translation regulators in cellular differentiation and carcinogenesis. *Biochim Biophys Acta Mol Basis Dis*. 2021;1867:166046.
- Gallo S, Ricciardi S, Manfrini N, Pesce E, Oliveto S, Calamita P, et al. Rack1 specifically regulates translation through its binding to ribosomes. *Mol Cell Biol*. 2018;38:e00230–18.
- Romano N, Di Giacomo B, Nobile V, Borreca A, Willems D, Tilesi F, et al. Ribosomal rack1 regulates the dendritic arborization by repressing fmrp activity. *Int J Mol Sci*. 2022;23:11857.
- Yoshino Y, Chiba N. Roles of rack1 in centrosome regulation and carcinogenesis. *Cell Signal*. 2022;90:110207.
- Cheng D, Zhu X, Barchiesi F, Gillespie DG, Dubey RK, Jackson EK. Receptor for activated protein kinase c1 regulates cell proliferation by modulating calcium signaling. *Hypertension*. 2011;58:689–95.
- Zhu X, Jackson EK. Rack1 regulates angiotensin ii-induced contractions of shr preglomerular vascular smooth muscle cells. *Am J Physiol Ren Physiol*. 2017;312:F565–F76.
- Suzuki H, Katanasaka Y, Sunagawa Y, Miyazaki Y, Funamoto M, Wada H, et al. Tyrosine phosphorylation of rack1 triggers cardiomyocyte hypertrophy by regulating the interaction between p300 and gata4. *Biochim Biophys Acta*. 2016;1862:1544–57.
- Kucherenko MM, Marrone AK, Rishko VM, Magliarelli Hde F, Shcherbata HR. Stress and muscular dystrophy: A genetic screen for dystroglycan and dystrophin interactors in drosophila identifies cellular stress response components. *Dev Biol*. 2011;352:228–42.
- Belozerov VE, Ratkovic S, McNeill H, Hilliker AJ, McDermott JC. In vivo interaction proteomics reveal a novel p38 mitogen-activated protein kinase/rack1 pathway regulating preostasis in drosophila muscle. *Mol Cell Biol*. 2014;34:474–84.
- Calura E, Cagnin S, Raffaello A, Laveder P, Lanfranchi G, Romualdi C. Meta-analysis of expression signatures of muscle atrophy: Gene interaction networks in early and late stages. *BMC Genomics*. 2008;9:630.
- Huttner SS, Ahrens HE, Schmidt M, Henze H, Jung MJ, Schuler SC, et al. Isolation and culture of individual myofibers and their adjacent muscle stem cells from aged and adult skeletal muscle. *Methods Mol Biol*. 2019;2045:25–36.
- Zecchini S, Giovarelli M, Perrotta C, Morisi F, Touvier T, Di Renzo I, et al. Autophagy controls neonatal myogenesis by regulating the gh-igf1 system through a nfe2l2- and ddit3-mediated mechanism. *Autophagy*. 2019;15:58–77.
- Forcina L, Cosentino M, Musaro A. Mechanisms regulating muscle regeneration: Insights into the interrelated and time-dependent phases of tissue healing. *Cells*. 2020;9:1297.
- Yoshimoto Y, Ikemoto-Uezumi M, Hitachi K, Fukada SI, Uezumi A. Methods for accurate assessment of myofiber maturity during skeletal muscle regeneration. *Front Cell Dev Biol*. 2020;8:267.
- Bi P, Yue F, Sato Y, Wirbisky S, Liu W, Shan T, et al. Stage-specific effects of notch activation during skeletal myogenesis. *eLife*. 2016;5:e17355.
- Gerrard JC, Hay JP, Adams RN, Williams JC 3rd, Huot JR, Weathers KM, et al. Current thoughts of notch's role in myoblast regulation and muscle-associated disease. *Int J Environ Res Public Health*. 2021;18:12558.

32. Chaturvedi D, Reichert H, Gunage RD, VijayRaghavan K. Identification and functional characterization of muscle satellite cells in drosophila. *eLife*. 2017;6:e30107.
33. Boukhatmi H. *Drosophila*, an integrative model to study the features of muscle stem cells in development and regeneration. *Cells*. 2021;10:2112.
34. Catalani E, Bongiorno S, Taddei AR, Mezzetti M, Silvestri F, Coazzoli M, et al. Defects of full-length dystrophin trigger retinal neuron damage and synapse alterations by disrupting functional autophagy. *Cell Mol Life Sci*. 2021;78:1615–36.
35. Boukhatmi H, Bray S. A population of adult satellite-like cells in drosophila is maintained through a switch in rna-isoforms. *eLife*. 2018;7:35954.
36. Bohnert KR, McMillan JD, Kumar A. Emerging roles of er stress and unfolded protein response pathways in skeletal muscle health and disease. *J Cell Physiol*. 2018;233:67–78.
37. Taylor MV, Hughes SM. Mef2 and the skeletal muscle differentiation program. *Semin Cell Dev Biol*. 2017;72:33–44.
38. Mitra S, Ryoo HD. The unfolded protein response in metazoan development. *J Cell Sci*. 2019;132:jcs217216.
39. Kershner L, Welshhans K. Rack1 regulates neural development. *Neural Regen Res*. 2017;12:1036–9.
40. Zhu Q, Chen L, Li Y, Huang M, Shao J, Li S, et al. Rack1 is essential for corticogenesis by preventing p21-dependent senescence in neural stem cells. *Cell Rep*. 2021;36:109639.
41. Vieira NM, Elvers I, Alexander MS, Moreira YB, Eran A, Gomes JP, et al. Jagged 1 rescues the duchenne muscular dystrophy phenotype. *Cell*. 2015;163:1204–13.
42. Bothe I, Baylies MK. *Drosophila* myogenesis. *Curr Biol*. 2016;26:R786–91.
43. Laurichesse Q, Soler C. Muscle development: A view from adult myogenesis in drosophila. *Semin Cell Dev Biol*. 2020;104:39–50.
44. Kadmas JL, Smith MA, Pronovost SM, Beckerle MC. Characterization of rack1 function in drosophila development. *Dev Dyn*. 2007;236:2207–15.
45. Volta V, Beugnet A, Gallo S, Magri L, Brina D, Pesce E, et al. Rack1 depletion in a mouse model causes lethality, pigmentation deficits, and reduction in protein synthesis efficiency. *Cell Mol Life Sci*. 2013;70:1439–50.
46. Yun J, Puri R, Yang H, Lizzio MA, Wu C, Sheng ZH, et al. Mul1 acts in parallel to the pink1/parkin pathway in regulating mitofusin and compensates for loss of pink1/parkin. *eLife*. 2014;3:e01958.
47. Wang Y, Melkani GC, Suggs JA, Melkani A, Kronert WA, Cammarato A, et al. Expression of the inclusion body myopathy 3 mutation in drosophila depresses myosin function and stability and recapitulates muscle inclusions and weakness. *Mol Biol Cell*. 2012;23:2057–65.
48. Chen W, Chen Y, Liu Y, Wang X. Autophagy in muscle regeneration: Potential therapies for myopathies. *J Cachexia Sarcopenia Muscle*. 2022;13:1673–85.
49. Kang K, Ryoo HD, Park JE, Yoon JH, Kang MJ. A drosophila reporter for the translational activation of atf4 marks stressed cells during development. *PLoS One*. 2015;10:e0126795.
50. Ryoo HD. *Drosophila* as a model for unfolded protein response research. *BMB Rep*. 2015;48:445–53.
51. Alter J, Bengal E. Stress-induced c/ebp homology protein (chop) represses myod transcription to delay myoblast differentiation. *PLoS One*. 2011;6:e29498.
52. Catalani E, Buonanno F, Lupidi G, Bongiorno S, Belardi R, Zecchini S, et al. The natural compound climacostol as a prodrug strategy based on ph activation for efficient delivery of cytotoxic small agents. *Front Chem*. 2019;7:463.
53. Catalani E, Fanelli G, Silvestri F, Cherubini A, Del Quondam S, Bongiorno S, et al. Nutraceutical strategy to counteract eye neurodegeneration and oxidative stress in drosophila melanogaster fed with high-sugar diet. *Antioxidants*. 2021;10:1197.
54. De Palma C, Morisi F, Pambianco S, Assi E, Touvier T, Russo S, et al. Deficient nitric oxide signalling impairs skeletal muscle growth and performance: Involvement of mitochondrial dysregulation. *Skelet Muscle*. 2014;4:22.
55. Giovarelli M, Zecchini S, Martini E, Garre M, Barozzi S, Ripolone M, et al. Drp1 overexpression induces desmin disassembling and drives kinesin-1 activation promoting mitochondrial trafficking in skeletal muscle. *Cell Death Differ*. 2020;27:2383–401.
56. Roux-Biejat P, Coazzoli M, Marrazzo P, Zecchini S, Di Renzo I, Prata C, et al. Acid sphingomyelinase controls early phases of skeletal muscle regeneration by shaping the macrophage phenotype. *Cells*. 2021;10:3028.
57. Chakraborty K, VijayRaghavan K, Gunage R. A method to injure, dissect and image indirect flight muscle of drosophila. *Bio-Protoc*. 2018;8:e2860.
58. Cazzato D, Assi E, Moscheni C, Brunelli S, De Palma C, Cervia D, et al. Nitric oxide drives embryonic myogenesis in chicken through the upregulation of myogenic differentiation factors. *Exp Cell Res*. 2014;320:269–80.
59. Giovarelli M, Zecchini S, Catarinella G, Moscheni C, Sartori P, Barbieri C, et al. Givinstat as metabolic enhancer reverting mitochondrial biogenesis deficit in duchenne muscular dystrophy. *Pharm Res*. 2021;170:105751.
60. Pambianco S, Giovarelli M, Perrotta C, Zecchini S, Cervia D, Di Renzo I, et al. Reversal of defective mitochondrial biogenesis in limb-girdle muscular dystrophy 2d by independent modulation of histone and pgc-1alpha acetylation. *Cell Rep*. 2016;17:3010–23.
61. Catalani E, Silvestri F, Bongiorno S, Taddei AR, Fanelli G, Rinalducci S, et al. Retinal damage in a new model of hyperglycemia induced by high-sucrose diets. *Pharm Res*. 2021;166:105488.

ACKNOWLEDGEMENTS

We are grateful to the Great Equipment Center (Università degli Studi della Tuscia) for providing access to microscopes. The Ph.D. student Silvia Rosanna Casati was supported by the Ph.D. program in Experimental Medicine of the University of Milan (Italy). The research has been supported by a grant from the Italian Ministry of University and Research (MUR), PRIN2020 to EClem/DC.

AUTHOR CONTRIBUTIONS

E Cat performed the experiments on *Drosophila* model and interpreted the data with the help of AC, SDQ, KB, FS, and SB. SZ and MG performed the experiments on mouse model and interpreted the data with the help of PRB, AN, and SRC. MC, NR, GP, E Clem, CP, and CDP analyzed/discussed the results, and contributed to the editing of the manuscript. DC conceived the study, designed the experiments, interpreted the data, and wrote the manuscript. All authors read and approved the final manuscript.

COMPETING INTERESTS

The authors declare no competing interests.

ADDITIONAL INFORMATION

Supplementary information The online version contains supplementary material available at <https://doi.org/10.1038/s41420-022-01250-8>.

Correspondence and requests for materials should be addressed to Davide Cervia.

Reprints and permission information is available at <http://www.nature.com/reprints>

Publisher's note Springer Nature remains neutral with regard to jurisdictional claims in published maps and institutional affiliations.



Open Access This article is licensed under a Creative Commons Attribution 4.0 International License, which permits use, sharing, adaptation, distribution and reproduction in any medium or format, as long as you give appropriate credit to the original author(s) and the source, provide a link to the Creative Commons license, and indicate if changes were made. The images or other third party material in this article are included in the article's Creative Commons license, unless indicated otherwise in a credit line to the material. If material is not included in the article's Creative Commons license and your intended use is not permitted by statutory regulation or exceeds the permitted use, you will need to obtain permission directly from the copyright holder. To view a copy of this license, visit <http://creativecommons.org/licenses/by/4.0/>.

© The Author(s) 2022